Theor Appl Climatol
DOI 10.1007/s00704-009-0206-x

ORIGINAL PAPER

Formulation of a tropical town energy budget (t-TEB) scheme

Hugo Abi Karam · Augusto José Pereira Filho · Valery Masson · Joël Noilhan · Edson Pereira Marques Filho

Received: 9 July 2008 / Accepted: 18 August 2009

Abstract This work describes the tropical town energy budget (t-TEB) scheme addressed to simulate the diurnal occurrence of the urban heat island (UHI) as observed in the Metropolitan Area of Rio de Janeiro (MARJ; −22° S; −44° W) in Brazil. Reasoning about the tropical urban climate have guided the scheme implementation, starting from the original equations from Masson (Bound-Lay Meteorol 94:357–397, 2000). The modifications include (a) local scaling approaches for obtaining flux–gradient relationships in the roughness sub-layer, (b) the Monin-Obukhov similarity framework in the inertial sub-layer, (c) increasing aerodynamic conductance toward more unstable conditions, and (d) a modified urban subsurface drainage system to transfer the intercepted rainwater by roofs to the roads. Simulations along 2007 for the MARJ are obtained and compared with the climatology. The t-TEB simulation is consistent with the observations, suggesting that the timing and dynamics of the UHI in tropical cities could vary significantly from the familiar patterns observed in mid-latitude cities—with the peak heat island intensity occurring in the morning than at night. The simulations are suggesting that the thermal phase shift of this tropical diurnal UHI is a response of the surface energy budget to the large amount of solar radiation, intense evapotranspiration, and thermal response of the vegetated surfaces over a very humid soil layer.

H. A. Karam (✉)
Departamento de Meteorologia,
Universidade Federal do Rio de Janeiro (IGEO-CCMN-UFRJ),
Bloco G, Sala G1-009, Av. Athos da Silveira Ramos, 274,
Cidade Universitária, Ilha do Fundão,
Rio de Janeiro, Rio de Janeiro, Brazil 21941 916
e-mail: hugo@igeo.ufrj.br

A. J. Pereira Filho
Departamento de Ciências Atmosféricas, Instituto de Astronomia,
Geofísica e Ciências Atmosféricas, Universidade de São Paulo,
Rua do Matão, 1226, Cidade Universitária,
05508-090 São Paulo, São Paulo, Brazil
e-mail: apereira@model.iag.usp.br

V. Masson · J. Noilhan
Groupe de Météorologie de Moyenne Echelle (CNRM/GMME),
Centre National de Recherches Météorologiques,
Météo-France, 42, av. Gustave Coriolis,
31057 Toulouse Cedex, France

V. Masson
e-mail: valery.masson@meteo.fr

J. Noilhan
e-mail: noilhan@meteo.fr

E. P. Marques Filho
Departamento de Meteorologia,
Universidade Federal do Rio de Janeiro (IGEO-CCMN-UFRJ),
Bloco G, Sala G1-014, Av. Athos da Silveira Ramos, 274,
Cidade Universitária, Ilha do Fundão,
Rio de Janeiro, Rio de Janeiro 21941 916, Brazil
e-mail: edson@igeo.ufrj.br

1 Introduction

The first generation of urban surface models used a "flat concrete slab" or a wet "sandbox" approach to represent the urban conditions (Best 2005). The touchstone conceptual element in surface energy budget (SEB) models is the urban canyon (UC) (Oke 1987). Due to the complexity of the urban surface, the urban SEB has received great attention, and many UC models were developed with successful results (Arnfield 1982; Grimmond et al. 1991; Grimmond and Oke (1991); Masson 2000; Kusaka et al. 2001; Martilli et al. 2002; Mestayer et al. 2005). One of the first urban SEB was the objective hysteresis model, dependent of a survey of the urban roughness elements (Grimmond et al.

Published online: 13 September 2009

1991). Two of the most complete parameterizations of the SEB and other urban effects to date are the town energy budget (TEB) scheme of Masson (2000) and the urban surface exchange parameterization of Martilli et al. (2002).

The TEB model is a physically based scheme representing the urban SEB associated with a set of UCs without a particular orientation. In this model, the SEB on urban surfaces (roofs, walls, and roads) is based on the solution of the first law of thermodynamics, considering geometric aspects of buildings, thermal and radiation properties to compute the surface fluxes, air temperature, and humidity. Otherwise, the Martilli's model computes multiple mixing scales associated with the distribution of UC, defining the turbulent fluxes based on the solution of the turbulent kinetic energy equation.

In recent years, applications of these schemes to simulate the urban boundary layer (UBL) of mid-latitude cities were done (Lemonsu and Masson 2002; Roulet et al. 2005). However, an inter-comparison is still necessary (Masson 2006).

There are a small number of observational and numerical investigations about the (sub)tropical UBL to date (Roth 2007), and consequently, the available knowledge about the tropical urban climate is very limited presently. The objective of this work to propose a tropical SEB scheme, usually called the tropical town energy budget (t-TEB) scheme. The starting equations used in t-TEB scheme were proposed by Masson (2000). However, several modifications were implemented in order to make the proposed scheme able to simulate the surface conditions of tropical cities.

This manuscript is divided into five sections: Section 2 presents the theoretical background, Section 3 describes the t-TEB scheme, Section 4 discusses the results, and Section 5 summarizes the conclusions.

2 Theoretical elements

The Monin–Obukhov similarity (MOS) theory framework permits the computation of turbulent fluxes in the surface layer (SL) under different stability conditions, using characteristic scales (Panofsky and Dutton 1984; Garratt 1980; Rotach 1995). The MOS theory assumes that, in quasi-stationary conditions over a horizontally homogeneous surface, the SL is constant flux layer. The urban SL is very complex, and the surface is not homogeneous. The result is that the urban SL can be divided in two sub-layers (Rotach 1995): a roughness sub-layer (RSL), where the turbulent fluxes are not constant along the vertical (where the MOS theory cannot be used), and an inertial sub-layer (ISL), where the characteristic scales can be determined by the MOS theory framework.

The RSL is the layer between the urban surfaces and the so-called *blending level*, z_*, with a range of values between 2.5 and five times the average height the roughness element (e.g., Roth and Oke 1993). Mahrt (2000) grouped the different formulations of the blending-height approach in a unified framework, which the general form of the blending height z_* can be expressed as $z_* = C\left(u_* U\right)^P w_c$, where u_* is the friction velocity, U the average wind speed at z_*, w_c the canyon width, and C and P are empirical coefficients usually taken as 1 and 2, respectively. In t-TEB, z_* is a simple function of the building height, z_b. In the ISL, there are empirical evidences for the partial validity of the MOS theory over complex surface (Roth 2000; Oke 2006; Marques Filho et al. 2008).

The methodology employed in the RSL is similar to the one used to find the universal normalized gradient functions under the MOS theory framework but with a local character (Raupach 1992). Therefore, the urban surface model is considering the MOS theory framework to obtain the universal characteristic scales u_*, T_*, and q_* in the ISL and the local scales u_f, T_f, and q_f in the RSL. These local scales cannot be confused with the local scales established by Nieuwstadt (1984) and Sorbjan (1986) for the stable BL. Additionally, simulating the tropical urban SL is necessary to consider the intensity of surface warming and the presence of free convection condition (Monin and Yaglom 1971, 1975; Grachev et al. 2000). The use of local scales in urban SEB is not new, and it is used to compute the fluxes in almost all urban surface parameterizations. For instance, Moriwaki and Kanda (2006) have evaluated the applicability of the flux–gradient relationships for momentum and heat for UBLs within the MOS theory framework. Other important aspect considered here is the hydrological budget in tropical urban areas. Masson (2000) considered unconstrained drainage system that is not able to simulate flooding over roads. Differently, a more realistic urban draining system was implemented in t-TEB scheme that is formally similar to the one proposed by Grimmond and Oke (1991), with a limited capacity of the urban drainage system. A comparison between the parameterizations utilized in the TEB and t-TEB scheme is given in Table 1.

3 The t-TEB scheme

3.1 Local scaling

In the UBL, the surface heterogeneities can induce spatial and temporal variability in the turbulent fluxes (Garratt 1980; Raupach 1992; Noilhan et al. 1997). In accord with Mahrt (2000), in the RSL, the turbulent transport has a local character, and the predictions of the MOS theory are no longer valid (Raupach and Finnigan 1997). In this case,

Table 1 Comparison between TEB and the t-TEB formulations

Approach	TEB (Masson 2000)	t-TEB
UC temperature	Only the divergence of Q_H	Divergences of Q_H and L_* (Nunez and Oke 1976)
Sensible heat flux	Modified flux-profile relationships in the SL (Mascart et al. 1995)	Local scaling in the RSL and the MOS theory in the ISL (Kastner-Klein and Rotach 2004)
Momentum flux	Idem above	Idem above
Latent heat flux	Idem above	Idem above plus the Penman-Monteith composed formulation (Monteith and Unsworth 2008)
Water budget	Infinite draining of the subsurface ducts	Limited draining of subsurface ducts (Grimmond and Oke 1991)
Internal temperatures	Explicit numerical scheme	Implicit numerical scheme: GTRID (Press et al. 1992)
External temperatures	Explicit scheme	Newton's relaxation
Sky-view factors	Noilhan (1981)	Oke (1987)
Infra-red irradiances	First order reflections	Multiply reflections (e.g. Arnfield and Mills 1994)
UC geometry	Canyon symmetry	Support a kind of UC asymmetry
Free convection	Polynomial approach of free convection (Mascart et al. 1995)	Asymptotic behavior of the MOS theory (Grachev et al. 2000)
Surface roughness and displacement	Constants (user defined)	Morphometric formulae (Kastner-Klein and Rotach 2004)

some empirical evidences have supported the application of the "local scaling" (e.g., Roth 2000; Belcher et al. 2003; Kastner-Klein and Rotach 2004). The local scales can be determined with bulk estimations of the fluxes near the different urban surfaces. Thus, the vertical profiles of the meteorological variables in RSL along the surfaces that define the UC prototype can be defined by integration of the following 'local gradient' equation:

$$\frac{\kappa\, x_i}{(\alpha_j)_f}\frac{\partial \alpha_j}{\partial x_i} = \varphi_f\left(\frac{x_i}{L_f}\right) \tag{1}$$

where α_j=u,T,q the extensive variables: wind speed, air temperature and specific humidity; x_i=x,y,z the spatial coordinates; $(\alpha_j)_f$ the local scale of α_j; κ the von Kármán constant; and L_f the local-length scale.

The ratio between the local scale of wind velocity in the RSL u_f and the friction velocity u_* of the ISL is obtained with the following empirical fitting curve (Kastner-Klein and Rotach 2004):

$$\frac{u_f}{u_*} = Z[\exp(2-2Z)]^{1/2} \tag{2}$$

$Z = \left(\frac{z-d_s}{z^*-d_s}\right)$ being a dimensionless height; $d_S = w_b h_b/(w_b + w_c)$ the average elevation of the surface composed by two-dimensional UC, and w_b and h_b the building width and height, respectively, and w_c the average road width. A constant-flux layer into the SL has been considered whose consequence is

$$\frac{T_f}{T_*} \approx \frac{q_f}{q_*} \approx \frac{\varphi_f}{\varphi} \approx \frac{u_*}{u_f} \tag{3}$$

Certainly, there is not much empirical evidence supporting the general validity of Eq. 3. The ratios are probably all smaller or larger than 1, but whether they are approximately equal at all heights (in the SL) is rather shaky.

The SL turbulent flow above very rough surfaces is dynamically influenced by the average roughness as well as by individual elements present on the urban surface. This layer presents very complex characteristics compared with the turbulent flow above smooth and horizontally homogeneous surfaces (Garratt 1980; Raupach et al. 1996; von Randow et al. 2002, 2006). In general, to express the action of a complex surface drag in the atmospheric flow, two aerodynamic parameters are used: the zero-plane displacement d and the roughness length z_0 (Thom et al. 1975). Pragmatically, the morphometric formulae from Kastner-Klein and Rotach (2004) are employed here,

$$\left(\frac{z_0}{h_b}\right) = 0.4\exp\left[-2.2\left(\lambda_p - 1\right)\right] + 0.6\lambda_p \tag{4}$$

$$\left(\frac{d}{h_b}\right) = 0.072\lambda_p\exp\left[-2.2\left(\lambda_p - 1\right)\right] \tag{5}$$

λ_p being the ratio between the building area and city area and is given by $\lambda_p = w_b/(w_b + w_c)$. Since the scales of d and z_0 have been specified, the variances and covariances in the RSL may be determined as functions of the local stability parameter, defined as $\zeta_f = (z-d)/L_f$, and local turbulent fluxes for the range of stability conditions $-2 \le \zeta_f \le 2$ (e.g., Roth and Oke 1993; Kaimal and Finningan 1994; Feigenwinter et al. 1999). In this study, the following criterion for defining the free convection

regime was considered, $\zeta_f < -2$, which is consistent with the proposition by Kader and Yaglom (1990).

In the t-TEB, an effective velocity u_{eff} is used to define the aerodynamic forcing of the model. The effective velocity forcing has two contributions: The first is from the mean wind velocity, sampled each 15 min by a weather station over the building roof, and the second is due to the variance of the fluctuations of wind velocity, which is not directly measured by conventional weather stations to date. These contributions are functions of the stability condition. The wind profile in the RSL (u_{RSL}) is computed by the matching expression proposed by Kastner-Klein and Rotach (2004):

$$u_{\text{RSL}}(z) = \frac{u*}{0.6\kappa}\left\{2.272 - \exp\left[0.6 - 0.072\left(\frac{z-d_0}{z_0}\right)\right]\right\} \tag{6}$$

$u*$ being the friction velocity in the ISL. The effective velocity u_{eff} is then obtained composing u_{RSL} with a high frequency fluctuation of the wind velocity.

The surface horizontal fluctuations are primarily controlled by the large convective motions in the convective boundary layer, following the mixed layer (ML) scaling down to the surface (Kaimal and Finnigan 1994; Marques Filho et al. 2008). In the ML, the appropriate height scale changes from u_f to $w*$ that is the convective velocity scale (Panofsky and Dutton 1984; De Bruin et al. 1993). In t-TEB scheme, a prognostic model after Tennekes' (1973) is used to determine the evolution of the ML height under convective conditions. In accord with Kaimal and Finningan (1994), "the fluctuations in the horizontal, being controlled primarily by the large convective motions in the convective BL, follow mixed layer scaling almost to the surface." Under convective conditions, an effective wind velocity is applied, as suggested by (Fairall et al. 1996; Grachev et al. 1997).

In the t-TEB, the drag effects of the urban canopy layer are described in a similar way the observed in forest canopy layers (Garratt 1994). The average of the horizontal wind speed through the azimuth directions, computed in the middle point inside the UC, has been defined by

$$u_{\text{can}}(z_b/2) = c_{\text{can}}\, u_{\text{eff}}(z_b)\exp(-n_1\zeta_1) \tag{7}$$

$\zeta_1 = 1 - z/z_b$ being the vertical coordinate above the canyon floor (road), u_{eff} (z_b/2) the effective wind speed in the middle point of the canyon, ζ_1=0.5, c_{can} an average azimuth factor, and n_1 is an UC shape factor equals to $n_1 \approx 0.5\alpha_c$ (Masson 2000), where $\alpha_c = (z_b/w_c)$ is the aspect ratio of the UC. The resulting u_{can} will depend on the flow adjustment above the urban roughness elements. Three types of adjusted flow expected were as follows: (a) the total flow separation, (b) the skimming flow, and (c) the UC vortex flow, all of them controlled by α_c. In t-TEB scheme, the coefficient c_{can} is given as proposed by Lemonsu et al. (2004),

$$c_{\text{can}} = \begin{cases} 1 & \text{if} \quad \alpha_c \le 1/2 \\ 1 + \left(\frac{4}{\pi} - 2\right)(\alpha_c - 0.5) & \text{if} \quad 1/2 < \alpha_c < 1 \\ 1/2 & \text{if} \quad \alpha_c \ge 1. \end{cases} \tag{8}$$

The general form of the surface fluxes, considering the arbitrary variable (A), is written in analogy with the Ohm's law (Beljaars 1994), i.e., $Q_A \approx -C_A(A_2 - A_1 r)/r_A$, being C_A a constant of proportionality and r_A the aerodynamic resistance. The aerodynamic resistances are determined by the iterative method (Thom 1975; Liu et al. 2007) considering the local gradients normal to the UC surfaces. The aerodynamic conductance (and resistance) is computed above the UC surfaces, considering the matching curve between the forced (Thom 1975) and free convection conditions (Grachev et al. 2000). A proper fit has been employed to maintain the continuity of the function along the full range of unstable conditions. The application of fitting curves over many evolving boundary conditions has been discussed by Shyy et al. (1996). In t-TEB, the flux–gradient relationships, under unstable conditions, are obtained with the following match,

$$\varphi = \varphi_i^{(1-\omega)}\varphi_f^{\omega} \tag{9}$$

where φ_i is the Thom's relationships for the normalized gradients of the MOS theory framework, φ_f is the relationships of Grachev et al. (2000) and $\omega = (2/\pi)atan(-\zeta)$ is the proposed exponential power weight. It is known that the tropical surfaces present a more wide range of unstable conditions (e.g., Marques Filho et al. 2008). During the summer period, the dry urban surface usually presents high temperatures, in the form of hot spots, and it is right to use semi-empirical flux–gradient relationships as proposed by Grachev et al. (2000). The comparison between the propositions for the aerodynamic conductivity is presented in Fig. 1. The proposed fit curves are continuous, very close to the Thom's curves at the beginning of the unstable condition ($-05 < \zeta < 0$) and progressively close to the curve of Viney (1991) for very unstable conditions. A potential increase of 20% in the sensible heat flux can be associated with the t-TEB approach under very unstable condition.

3.2 Temperature and humidity equations

The urban SEB depends of the external and internal temperature of the roughness elements in the surface. The canyon surface temperature presents three compo-

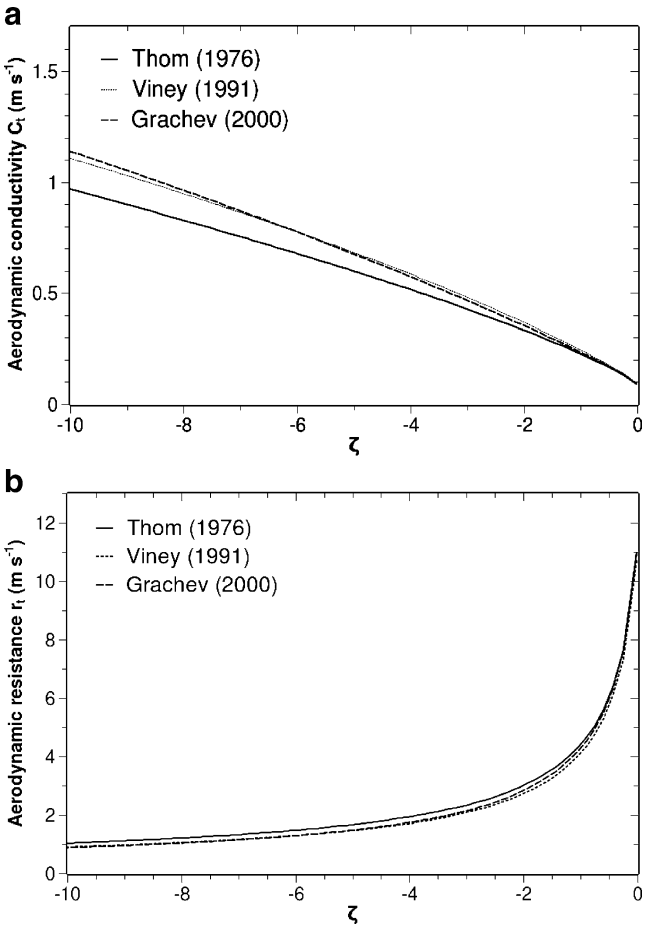

Fig. 1 Comparison between **a** aerodynamic conductivities and **b** aerodynamic resistances for heat transport under unstable conditions

nents: substrate temperature, external temperature, and canyon air temperature. The time evolution of the substrate temperature T_{sub} for roofs, walls, and roads is obtained with the Fourier heat conduction equation that is written as

$$\frac{\partial T_{\text{sub}}}{\partial t} = -\nu \frac{\partial Q_{\text{G}}}{\partial z} \tag{10}$$

being ν the thermal diffusivity of the conductive matter of the surface, $Q_G = -\gamma(\partial T_{\text{sub}}/\partial z)$ the heat flux and γ the thermal conductivity. A numerical solution in finite differences is carried out by the Thomas' Three-Diagonal Matrix algorithmic (Roach 1972; Press et al. 1989). The external temperatures employ the SEB equation (Oke 1987) given by

$$f(T)_i = \left(R_* - Q_{\text{G}} - Q_{\text{H}} - Q_{\text{E}}\right)_i = 0 \tag{11}$$

where $(T)_i$ is the external temperature of the ith surface (without energy storage), the subscript i represents the roofs, walls or roads; R_* is the net irradiance; Q_{G} is the molecular heat conduction from the exterior of the surface to its interior; Q_{H} an Q_{E} are the sensible and latent heat fluxes, respectively, for each surface. The numerical solution is achieved by a successive relaxation method (Marchuk 1974),

$$T_i^{(n+1)} - T_i^{(n)} + \alpha_n f\left(T_i^{(n)}\right) = \varepsilon \tag{12}$$

α_n being the relaxation factor, and ε, called the residual, a measure of the error of the guess of the nth order in the successive estimation. The Newton–Rapson's method is employed to compute α_n.

The canyon temperature T_{can} is driven by the entrainment of the urban BL air into the UC, by the anthropogenic flux of heat and humidity, and by the divergence of the radiation (infrared) density flux through the surfaces of the UC (Fuggle and Oke 1976; Nunez and Oke 1976). Here, T_{can} is considered as the average temperature in the air volume of the UC (Fig. 2a). Using the divergent

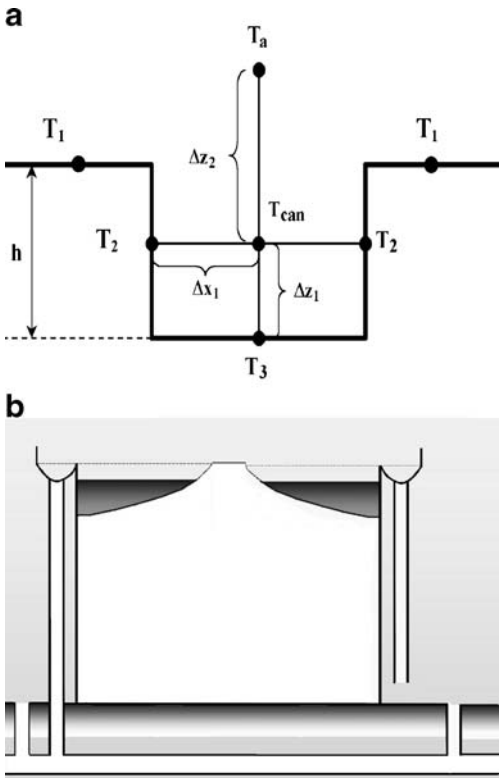

Fig. 2 Distribution of temperature on the symmetrical UC over a horizontal terrain (**a**), being T_1, T_2, and T_3 the average roof, wall, and road temperatures, respectively; T_{can} the mean internal canyon air temperature; T_{a} the air temperature above the canopy layer; Δz and Δx are the vertical and horizontal displacements, respectively; and h the building height. In **b**, the roof water reservoir as proposed by Masson (2000) (lhs) and the proposed t-TEB reformulation (rhs). The dimensions of surface reservoirs on the roof are much exaggerated to facilitate their visualization in the figure

theorem and the first law of thermodynamic, the time evolution of T_{can} is given by

$$aV\frac{\partial T_{can}}{\partial t} = -\int\int\int_V \nabla\cdot\left(\overrightarrow{Q}_H + \overrightarrow{Q}_A + \overrightarrow{Q}_R\right) dV \quad (13)$$

In Eq. 13, V represents the canyon air volume, ρ_a is the air density (assumed constant), c_p is the specific heat at constant pressure of the air, $\overrightarrow{Q}_H$ is the turbulent heat flux density from the walls and surfaces of the canyon, $\overrightarrow{Q}_A$ is the anthropogenic heat flux density, and $\overrightarrow{Q}_R$ is the net radiation flux density. This equation has been solved numerically by a finite difference method, backward in time and centered in space (Mesinger and Arakawa 1979). In accord with Mills (1997), empirical evidences shows that the air in the UC is almost isothermal, except near to surfaces where the gradient temperatures is important, and the temperature can differ by 2°C from the rest of the air volume (Arnfield and Mills 1994; Nakamura and Oke 1988). Different approaches to estimate $\overrightarrow{Q}_A$ are available in the literature (e.g., Matsuura 1995; Oke 1987; Sailor and Lu 2004). However, $\overrightarrow{Q}_A$ measures are quite unavailable in tropical cities, and it is neglected in the numerical realization forward.

A similar approach to the temperature is used for computing the evolution of the specific air humidity (q_{can}) inside the UC. The associated prognostic equation for q_{can} is presented as following

$$c_E V\frac{\partial q_{can}}{\partial t} = -\int\int\int_V \nabla\cdot\left(\overrightarrow{Q}_E + \overrightarrow{Q}_{EA}\right) dV \quad (14)$$

where $\overrightarrow{Q}_E$ is the turbulent water vapor flux determined locally; Q_{AE} is the anthropogenic water vapor flux released inside the UC, given by a single harmonic function with amplitude of 1(W m^{-2}); $c_E=\rho_a L_v$ is assumed constant here; and L_v is the latent heat of condensation. This equation is solved numerically by a finite difference method, backward in time and centered in space (Mesinger and Arakawa 1979).

3.3 Trapped infrared irradiance

In the t-TEB scheme, the successive reflections of infrared irradiances between the UC surfaces were implemented. The number of successive reflections can be used to define the hierarchy order of radiative interactions. It is an exercise to define the series of reflections between two surfaces, named i and j, for an (a)symmetrical UC, which results

$$\Delta L_i^* = -\left(\overline{\epsilon}_i\sigma\overline{T}_i^4\right)\sum_{j=1}^{4}\left[\frac{1-\Psi_{ij}\Psi_{ji}(1-\epsilon_i)}{1-\Psi_{ij}\Psi_{ji}(1-\epsilon_i)(1-\epsilon_j)}\right](1-\delta_{ij}) + \sum_{j=1}^{4}\left(\overline{\epsilon}_j\sigma\overline{T}_j^4\right)\left[\frac{\Psi_{ij}\epsilon_i}{1-\Psi_{ij}\Psi_{ji}(1-\epsilon_i)(1-\epsilon_j)}\right](1-\delta_{ij}) \quad (15)$$

where Ψ_{ij} is the sky-view factor associated with the view of surface j from the medial point of surface i. In Eq. 15, the first term in the rhs is the irradiation due to the surface i and the second term due to the surface j. The first term also represents the net thermal infrared emission by the ith surface, followed by an infinite number of reflections with the surfaces jth, discarding the combinations $i=j$. The second term also represents the net flux density of thermal infrared (IR) on the ith surface associated with the emission of jth surface, followed by an infinite number of reflections between them. The subscript j=0, 1, 2, 3, or 4 indicates the surfaces: (0) to the sky, which is controlled by first layer of humid air above the surface (Unsworth and Monteith 1975), (1) to the roofs, (2) to the left walls, (3) to the roads, and (4) to the right walls. It is worth to note that, for asymmetrical canyons, the IR irradiances of surfaces 2 and 4 (the walls) can differ significantly. The details of the derivation of the net IR irradiation correspond to geometric progression series exercises (and it is not shown). The over bar represent the mean surface value because the surface is occasionally covered by liquid water. Considering all sources, the net thermal IR irradiation of surface i can be expressed by the following equation:

$$L^*{}_i = L\downarrow\overline{\Psi}_{i0}\overline{\epsilon}_i - \overline{\epsilon}_i L\downarrow\sum_{j=1}^{4}\left[\overline{\Psi}_{i0}(1-\overline{\epsilon}_j)\overline{\Psi}_{ij}(1-\delta_{ij})\right] - \overline{\epsilon}_i\sum_{j=1}^{4}\left[(1-\delta_{ij})\overline{\Psi}_{ij}\sum_{k=1}^{4}\left[(1-\delta_{kj})\left(_k\sigma\overline{T}_k^4\right)\overline{\Psi}_{jk}(1-\overline{\epsilon}_j)\right]\right] - \Delta L_i^* \quad (16)$$

Equation 16 is associated with a target/source problem. The first term at the rhs represents the fraction of the atmospheric thermal IR irradiation absorbed by surface i and that is composed by the contribution from the sky, minus the reflection by the surface backward, which is given by: $L\downarrow\overline{\Psi}_{i0} - L\downarrow\overline{\Psi}_{i0}(1-\overline{\epsilon}_i) = L\downarrow\overline{\Psi}_{i0}\overline{\epsilon}_i$. The second term represents the contribution of the first-order reflection by the surfaces j of the sky irradiance reflected by the i surface. The third term represents the thermal IR irradiation emitted by surface k, reflected on the j surface,

and finally absorbed by the i surface. The last term represent emissions and multiple reflections between the surface pairs. Again, the derivation is an exercise considering the geometric progression series with infinity terms. Therefore, the equation considers infinity possibilities of emissions and reflections between surface pairs. On this way, the symmetry hypothesis may be relaxed, since the all the surfaces i iterations are explicitly considered. Note that Masson (2000) implemented only the first-order reflections for a symmetrical UC. In the t-TEB scheme, the global irradiation is obtained by the sum of direct and diffuse components of shortwave (SW) and long-wave (LW) irradiances, both upward and downward components (Unsworth and Monteith 1975; Unsworth 1975; Liou 2002). The sky-view factor Ψ_{ij} is defined as the fraction of the irradiance incoming through the solid angle, of the observed sky, from the point of view of the middle point of a given receptive surface. The mean surface parameter Ψ_{ij} can be calculated including the effects of lateral asymmetries (not shown). In this work, the usual co-sin dependent sky-view for symmetrical canyons (Oke 1987) is employed.

3.4 Water budget equations

The employment of the Penman–Monteith's formulation (PM) to compute the latent heat flux over cities was proposed by Grimmond and Oke (1991, 2002). The PM formulation has received great attention since it is able to compute of surface evapotranspiration over a full range of vegetated surfaces (Monteith and Unsworth 2008). The PM can be considered as the result of two approaches: (1) the Bowen ratio energy balance methodology, and (2) aerodynamic bulk approach (Oke 1987).

In the t-TEB scheme, the PM is employed (Karam and Pereira Filho 2006). The urban surfaces should be considered a storm-water reservoir of limited capacity. In the t-TEB scheme, it is supposed that no more than 10% of the surface area should be occupied by the storm-water reservoir, without transfer the outgoing flow directly to the urban drainage system. Only after the reservoirs are completed, the water excess (or runoff) can be transferred to the subsurface draining ducts and channels. Particularly, the roofs are able to drain rapidly the excess of water that overpasses their capacity of retention and transfer the excess to the roads. In the case of the majority of the tropical cities, the water in excess from the roofs will fall out directly over the roads, increasing the resulting incoming of water over this "lower" surface of the city. These ideas were implemented in the t-TEB scheme in order to determine the time evolution of the water accumulation over roofs and roads (Fig. 2b).

A variable draining ratio is considered by the t-TEB scheme. The hydrological balance, based on Grimmond and Oke (1991), is written as following,

$$\frac{\partial W_i}{\partial t} = P_i\left(1 + f_{ji} - f_{ij}\right) - D_i - \frac{(Q_E)_i}{L_v} \tag{17}$$

W_i being the running water balance over the surface i, in (kg m^{-2}s^{-1}), P_i the rainfall rate in the same unit, f_{ij} and f_{ji} the proportion of rain arrived at or diverted from the surface i to another surface j (e.g., f_{13} is a pipe water supply diverting water from the roof to the road), Di the mean urban draining rate along the surface, and $(Q_E)i$ the net latent heat flux (evaporation minus condensation).

In the rhs of Fig. 2b, the illustration of the roof reservoir employed in the t-TEB scheme is indicated (at the roof level of the building). The can-like container of the roof proposed in the TEB scheme by Masson (2000) is presented on the lhs of Fig. 2b, too. In the TEB scheme, the drainage ducts are supposed to have a very large capacity, and the excess of water is rapidly drained. Differently, in the t-TEB scheme, the draining process is limited. In the TEB scheme, the excess of rainwater overflows, and it is discharged into the underground channel. In the t-TEB scheme, the corresponding excess of water is first released over the roads, contributing to the road reservoir inflow, and drains slowly to the underground channel. Therefore, when the rainfall is large enough, the water can flood on prone areas. The order of magnitude of the urban drainage flux from a paved surface is almost 1.4 kg m^{-2}h^{-1}, corresponding to a 100 mm h^{-1} of rainfall incoming on a flat surface, as recommended by the literature (Hall 1984; Grimmond and Oke 1991; Akan 1993). The drainage D_i is computed as suggested by Grimmond and Oke (1991):

$$\begin{aligned} D_i^{0.333} &= \{W_i - \mathrm{C}_i\}/\tau_d \quad \text{if} \quad W_i > \mathrm{C}_i \\ D_i &= 0 \quad \text{if} \quad W_i \le \mathrm{C}_i \end{aligned} \tag{18}$$

C_i being the surface water capacity (kg m^{-2}) and τ_d the drainage time scale. The underground set of ducts is able to send the conveyed water downward to the chief channel (e.g., a river), but the flow is limited by the subsurface ducts capacity. For Grimmond and Oke (1991), an acceptable value of the drainage time scale is close to one-half hour ($\tau_d \approx 1{,}671$ s). The runoff and the bare soil infiltration are not represented in the present version of the scheme, since the town surface is supposed flat and impervious.

4 Numerical simulations

4.1 Accessing the parameter sensibility

The efficiency of parameter calibration would clearly be enhanced if it was possible to concentrate the effort on

those parameters to which the model simulation results are most sensible (Beven 2002). To obtain this information, we investigate the sensitivity of the input parameters used in the t-TEB scheme. The sensitivity of the model simulation can be defined with respect to a performance measure, e.g., the canyon temperature, the town sensible heat flux, etc., actually simulated by the t-TEB scheme. In order to assess the parameter sensitivity of the model simulation results, sensitivity to a particular parameter can be defined by the local gradient of the response surface in the direction of the chosen parameter axis. A sensitivity index can be defined as following,

$$S_{ij} = \frac{\partial Z_j}{\partial x_i} \tag{19}$$

S_{ij} being the sensitivity index with respect to the parameter i with value x_i and Z_j the value of the variable (or performance measure j at that point in the parameter space) (McCuen 1973). In this work, a normalized mean square root sensitivity index (σ_{ij}) is computed as

$$\sigma_{ij} = \frac{1}{n-1}\left[\sum_{t=1}^{n}\left(\frac{1}{Z_j}\frac{\partial Z_j}{\partial x_i}dx_i\right)^2\right]^{1/2} \tag{20}$$

where n is the total number of the outputs of the model. The performance measure used for assessing the parameter sensitivity of the t-TEB model simulation is generally a prognostic variables (urban surface temperatures, specific humidity, urban heat fluxes, etc.), or indeed, a related cumulative variable, as such the mixture layer height for the convective BL or the heat storage. As suggested by Beven (2002), the local gradients are evaluated numerically by a finite difference scheme, i.e., evaluating the change in Z as x_i changed by an enough small amount (e.g., 1%). The Euler's forward scheme was employed (Mesinger and Arakawa 1979) in the evaluation in the immediate region of the estimated "optimum" parameter set after a subjective exercise of chose.

The METAR data at the Santos Dumont's Airport (METAR code SBRJ) on the Metropolitan Area of Rio de Janeiro (MARJ) in the Southeastern part of Brazil, from a clear day of February 2007, was used to define the atmospheric forcing of the t-TEB scheme during the sensibility analysis realizations. Note that the Rio's airport is located in the MARJ, 2 km near the downtown. A simulation of 24 h was realized for assessing the parameter sensibility. A set of 93 simulations were realized considering small variations of the input parameters. Then, the output sensitivity is discussed for all parameters and performance measures (both prognostic and diagnostic output variables from t-TEB results). A number of 106 sensitivity output performance variables for 93 model input parameters were analyzed and organized following a crescent order of the sensitivity index.

The analysis shows a complex behavior of the model sensitivity to the parameter variations. The expected strong impact on the sensible heat flux of the roof and on the other SEB components on the UC surfaces was verified. In relation to the UC surface radiation budget, the performance variables seem to be more sensitive to the emissivity than to the surface albedo (for small variations).

The most important geometric parameter emerging from the analysis is the aspect ratio, due to the wide sensitivity of the performance variables in relation to the building height. The UC SEB is sensitive to the initial values of the surface temperatures. Especially, the surface temperature of walls and roads are more effective than the roof surface temperature, i.e., to produce variations in the modeled SEB. The internal temperature of the surface material presents only a relatively small impact on the sensitivity of the variables performance. However, the results are really very sensible to the composition material of the buildings and roads, as showed by the relative impacts of the associated thermal capacity and conductivity. In addition, it is sensitive also to the internal distribution of the materials in the roofs, walls, and roads layers. This find is almost unsuspected since is it very difficult to evaluate the efficiency of the urban materials as good thermal isolator "a priori", i.e., without considering the relative role of the assembled material in layers.

4.2 Simulation of the UHI of Rio de Janeiro City

The diurnal characteristics of the Rio de Janeiro's UHI have been described by Marques Filho et al. (2009), in a pattern that is distinctly different from what has been commonly observed in mid-latitude cities; the tropical UHI in the MARJ occurs during the morning and not during the night. The particular feature has been attributed to the large availability of solar irradiation and to the differences in the thermal wave phase shift due to the heterogeneities along the MARJ.

The comparison between the observed and simulated tropical UHI to the MARJ is showed in Figs. 3 and 4. The urban surface was simulated with t-TEB scheme and the vegetated suburban with the big-leaf scheme proposed by Deardorff (1978). The analysis of the simulation UHI obtained with t-TEB and big-leaf schemes has supported the temperature wave displacement toward late afternoon, as observed in the data series. It is considered that the displacement of the diurnal cycle of temperature is due to the force restoration driven by the second layer of soil, especially for quite saturate conditions beneath the vegetated suburban.

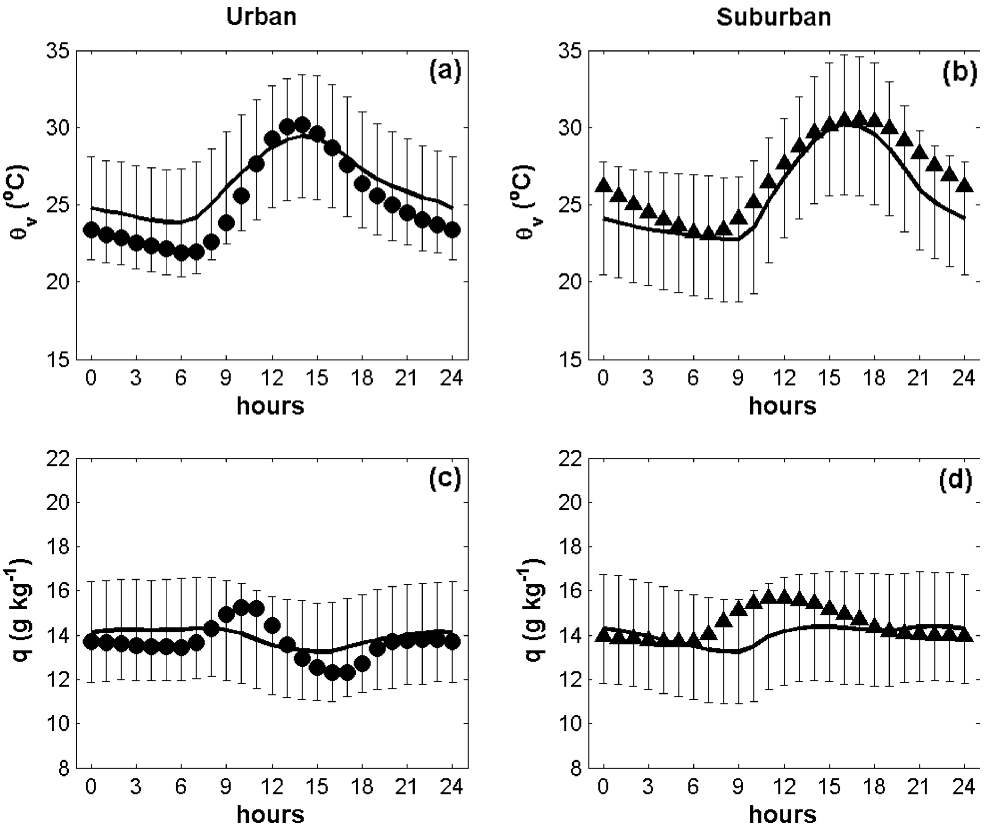

Fig. 3 Comparison between mean observations (*bold lines*) and mean simulations (*symbols*) with t-TEB along 2007. The graphics show the average diurnal evolution of the potential temperature (**a**, **b**) and the specific humidity (**c**, **d**). Results for urban (lhs) and suburban (rhs) areas of MARJ are presented. The *vertical bars* indicate the standard deviation of observations

4.3 Surface water balance

It is necessary to talk about the urban water budget in the context of the urban SEB. The accumulation of water over the urban surfaces is able to influence both the SEB as also the surface water balance. In accord with Beven (2002), the urbanization has a significant effect on rainfall–runoff relationships, but almost all the integrated models to date have taken very little explicit account of urban areas in their rainfall–runoff predictions. Some effort has been realized in the Institut National Polytechnique de Grenoble (e.g., Morena 2004) to simulate the water storage into the urban soil. On the other hand, some advances in coupling land surface models and hydrological models for flash flood forecasting, with horizontal resolution up to 2.5 km, have been realized by Vincendon et al. (2009). The scheme t-TEB has larger capacity of water accumulation over the urban surfaces. Actually, the discharge of the water excess

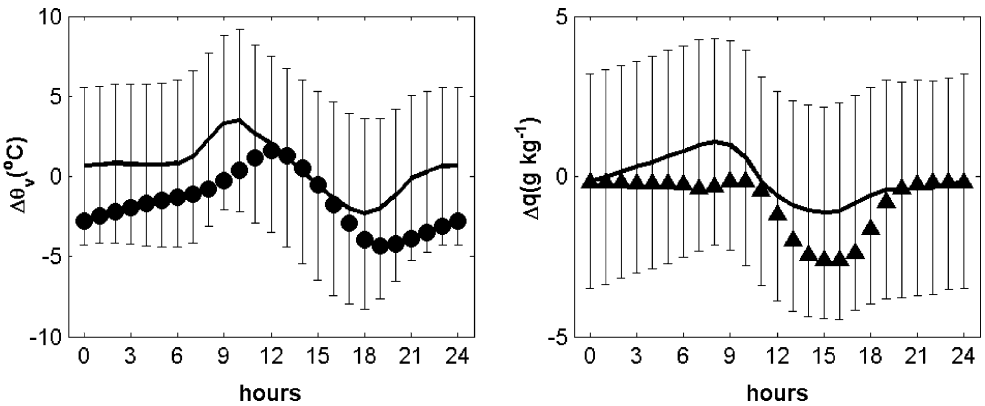

Fig. 4 Comparison of the UHI of Rio de Janeiro City, in Brazil, as observed (lhs) (*bold lines*) and simulated by t-TEB minus big-leaf (*symbols*) along 2007. The *curves* and *points* represent the hourly evolution of the virtual potential temperature differences (lhs) and the specific humidity differences (rhs). The *vertical bars* indicate the standard deviation of observations

from the surface reservoirs is limited (unlimited) in present versions of t-TEB (TEB). Comparing t-TEB and TEB, it was observed that the difference into the evapotranspiration is lower than 10% for the annual cycle. However, the rainfall can be enough to generate a large amount of accumulation over the urban surfaces under convective rainstorms (Pereira Filho et al. 2008). Integrated to mesoscale models, the urban surface scheme can be used as a tool of a hydrometeorological prediction center.

5 Conclusions and perspectives

In this work, the main equations of a new tropical urban surface scheme were described. The new scheme called t-TEB can be considered an updated revision of the TEB scheme (Masson 2000), particularly addressed to simulate the tropical urban climates. In this work, the new scheme is employed to simulate the SEB of Rio de Janeiro City, in Brazil, along the year of 2007.

The t-TEB scheme implements a local scaling framework to compute the UC emerging fluxes, including (i) a more intense diffusion under free convection conditions and (ii) a limited urban drainage system, which is able to modulate the water accumulation over the roads of the tropical city. The guide idea of the new approach was to improve the description of the SEB of tropical cities. The t-TEB simulation is able to simulate the annual evolution of surface variables within a standard deviation of the observed hourly mean.

Marques Filho et al. (2009) have discussed original finding on the UHI of the tropical Rio de Janeiro City, in Brazil, suggesting that the timing and dynamics of the UHI in tropical cities could vary significantly from the familiar patterns observed in mid-latitude cities—with the peak heat island intensity occurring in the morning than at night.

The simulation with the t-TEB and big-leaf schemes along 2007 is supporting the diurnal occurrences of the UHI of Rio de Janeiro City. The causes of the diurnal occurrence of the tropical UHI of Rio the Janeiro is likely associated to (1) the large incoming of solar radiation mainly used to warming the urban surfaces during the daytime, (2) the presence of vegetated areas in the suburbs, with consequence in the evapotranspiration intensity, and (3) the drift of the phase of the thermal wave above vegetated suburban surfaces that occurs in association with the force restoration of the surface temperature. The urban and suburban surfaces present similar SEB in Rio de Janeiro City, resulting in a Bowen ratio around 1 during the daytime.

The simulations realized to date is addressing the t-TEB scheme for coupling with mesoscale and large eddy simulation models, allowing further investigations of the 3D structure of the urban BL.

Acknowledgments The authors thank to the Centre National de Recherches Météorologiques (MétéoFrance), Instituto de Astronomia, Geofísica e Ciências Atmosféricas (USP), Fundação de Amparo à Pesquisa do Estado de São Paulo (FAPESP), Coordenação Nacional de Pesquisa e Desenvolvimento Científico (CNPq), and Instituto de Geociências (IGEO/UFRJ).

References

Akan AO (1993) Urban stormwater hydrology: a guide to engineering calculations. CRC, Boca Raton, p 265

Arnfield AJ (1982) An approach to the estimation of the surface radiative properties and radiation budgets of cities. Phys Geogr 3:97–122

Arnfield AJ, Mills GM (1994) An analysis of the circulation characteristics and energy budget of a dry, asymmetric, east-west urban canyon II. Energy budget. Int J Climatol 14:239–261

Belcher SE, Jerram N, Hunt JCR (2003) Adjustment of a turbulent boundary layer to a canopy of roughness elements. J Fluid Mech 488:369–398

Beljaars ACM (1994) The parametrization of surface fluxes in large-scale models under convection. Q J Roy Meteor Soc 121:225–270

Best MJ (2005) Representing urban areas within operational numerical weather prediction models. Bound-Lay Meteorol 114:91–109

Beven KJ (2002) Rainfall–runoff modelling—the primer. Wiley, Chichester, p 360 ISBN 978-0-470-86671-9

De Bruin HAR, Kohsiek W, Van Den Hurk JJM (1993) A verification of some methods to determine the fluxes of momentum, sensible heat, and water vapor using standard deviation and structure parameter of scalar meteorological quantities. Bound-Lay Meteorol 63:231–257

Deardorff JW (1978) Efficient prediction of ground surface temperature and moisture, with inclusion of a layer of vegetation. J Geophys Res-Atmos 83(C4):1889–1903

Fairall CW, Bradley EF, Rogers DP, Edson JB, Young GS (1996) Air-sea flux parameterization in TOGA COARE. J Geophys Res-Atmos 101(C2):3747–3764

Feigenwinter C, Vogt R, Palow E (1999) Vertical structure of selected turbulence characteristics above an urban canopy. Theor Appl Climatol 62:51–63

Fuggle RF, Oke TR (1976) Long-wave radiative flux divergence and nocturnal cooling of the urban atmosphere. I: Above Roof-Level. Bound-Lay Meteorol 10:113–120

Garratt JR (1980) Surface Influence upon vertical profiles in the atmospheric near-surface layer. Q J Roy Meteor Soc 106:803–819

Garratt JR (1994) The atmospheric boundary layer. Cambridge Atmospheric and Space Science Series, Cambridge, p 316

Grachev AA, Fairall CW, Zilitinkevich SS (1997) Surface-layer scaling for the convection-induced stress regime. Bound-Lay Meteorol 83:423–439

Grachev AA, Fairall CW, Bradley EF (2000) Convective profile constants revisited. Bound-Lay Meteorol 83:423–439

Grimmond CSB, Oke TR (1991) An evapotranspiration-interception model for urban areas. Water Resour Res 27(7):1739–1755

Grimmond CSB, Oke TR (2002) Turbulent heat fluxes in urban areas: observations and a local-scale urban meteorological parameterization scheme (LUMPS). J Appl Meteorol 41(7):792–810

Grimmond CSB, Cleugh HA, Oke TR (1991) An objective urban heat storage model and its comparison with other schemes. Atmos

Environ B-Urb 25(3):311–326 Objective Hysteresis Model (OHM)
Hall MJ (1984) Urban hydrology. Elsevier, Essex, p 310
Kader BA, Yaglom AM (1990) Mean fields and fluctuation moments in unstably stratified turbulent boundary layers. J Fluid Mech 212:637–662
Kaimal JC, Finningan JJ (1994) Atmospheric boundary layer flows—their structure and measurements. Oxford University Press, New York, p 289
Karam HA, Pereira Filho AJ (2006) Revisão dos métodos de Penman e Penman Monteith aplicado aos cânions urbanos. Rev Brasil Meteorol 21(1):86–106 In Portuguese
Kastner-Klein P, Rotach MW (2004) Mean flow and turbulence characteristics in an urban roughness sublayer. Bound-Lay Meteorol 111:55–84
Kusaka H, Kondo H, Kikegawa Y, Kimura F (2001) A simple single-layer urban canopy model for atmospheric models: comparison with multi-layer and slab models. Bound-Lay Meteorol 101:329–358
Lemonsu A, Masson V (2002) Simulation of a summer urban breeze over Paris. Bound-Lay Meteorol 104:463–490
Lemonsu A, Grimmond CSB, Masson V (2004) Modelling the surface energy budget of an old Mediterranean city core: Marseille. J Appl Meteorol 43:312–327
Liou KN (2002) An introduction to atmospheric radiation. International Geophysics Series, 2nd edn, Elsevier, Amsterdam, p. 583
Liu S, Lu L, Mao D, Jia L (2007) Evaluating parameterizations of aerodynamic resistance to heat transfer using field measurements. Hydrol Earth Syst Sci 11:769–783
Mahrt L (2000) Surface heterogeneity and vertical structure of the boundary-layer. Bound-Lay Meteorol 96:33–62
Marchuk GI (1974) Numerical methods in weather prediction [*Chislennye letody v prognoze pogody*, trans. Trirogoff and VR Lamb]. Academic, New York, p. 277
Marques Filho EP, Sá LD, Karam HA, Alvara RM, Souza A (2008) Atmospheric surface layer characteristics of turbulence above the Pantanal wetland regarding the similarity theory. Agr Forest Meteorol 148(6–7):883–892
Marques Filho EP, Karam HA, Miranda AG, Franca JRA (2009), Rio de Janeiro's urban climate. Urban Climate News—Quarterly Newsletter of the International Association of Urban Climate (IAUC), issue no. 32, June, 5–9. http://www.urban-climate.org
Martilli A, Clappier A, Rotach MW (2002) An urban surface exchange parameterization for mesoscale models. Bound-Lay Meteorol 104:261–304
Mascart P, Noilhan J, Giordani H (1995) A modified parameterization of flux-profile relationship in the surface layer using different roughness length values for heat and momentum. Bound-Lay Meteorol 72:331–344
Masson V (2000) A physically-based scheme for the urban energy budget in atmospheric models. Bound-Lay Meteorol 94:357–397
Masson V (2006) Urban surface modeling and the mesoscale impact of cities. Theor Appl Climatol 84:35–45
Matsuura K (1995) Effects of climate change on building energy consumption in cities. Theor Appl Climatol 51:105–117
McCuen RH (1973) The role sensitivity analysis in hydrologic modelling. J Hydrol 18:37–53
Mesinger F, Arakawa A (1979) Numeric methods used in atmospheric models. GARP Publications Series no. 17, vol. 1, Aug. 1979 (reprinted Nov. 1982). AMS/WMO, p 64
Mestayer PG, Durand P, Augustin P, Bastin S, Bonnefond J-M, Bénech B, Campistron B, Coppalle A, Delbarre H, Dousset B, Drobinski P, Druilhet A, Fréjafon E, Grimmond CSB, Groleau D, Irvine M, Kergomard C, Kermadi S, Lagouarde J-P, Lemonsu A, Lohou F, Long N, Masson V, Moppert C, Noilhan J, Offerle B, Oke TR, Pigeon G, Puygrenier V, Roberts S, Rosant J-M, Saïd F, Salmond J, Talbaut M, Voogt J (2005) The urban boundary-layer field campaign in Marseille (UBL/CLU-ESCOMPTE): set-up and first results. Bound-Lay Meteorol 114:315–365
Mills G (1997) An urban canopy-layer climate model. Theor Appl Climatol 57:229–244
Monin AS, Yaglom AM (1971) Statistical fluid mechanics. Volume I: mechanics of turbulence. Dover, New York, p 769 ISBN 0-486-45883-0 (v. 1 pbk)
Monin AS, Yaglom AM (1975) Statistical fluid mechanics. Volume II: mechanics of turbulence. Dover, New York, p 874 ISBN 0-486-45891-0 (v. 2 pbk)
Monteith JL, Unsworth MH (2008) Principles of environmental physics, 3rd edn. Elsevier, New York. ISBN 978-0-12-505103-3
Morena F (2004) Modelisation Hydrologique Distribuee en Milieu Urbanise—representation des processus de production et development du modele URBS. PhD thesis, Laboratoire Central des Ponts et Chaussees. Institut Nacional Polytechnique de Grenoble, France, p 257
Moriwaki R, Kanda M (2006) Flux-gradient profiles for momentum and heat over an urban surface. Theor Appl Climatol 84:127–135
Nakamura Y, Oke TR (1988) Wind, temperature and stability conditions in an east-west oriented urban canyon. Atmos Environ B-Urb 22:2691–2700
Nieuwstadt FTM (1984) Turbulence structure of the stable nocturnal boundary layer. J Atmos Sci 41:2202–2216
Noilhan J (1981) A model for the net total radiation flux at the surface of a building. Build Environ 16:269–266
Noilhan J, Lacarrère P, Dolman AJ, Blyth EM (1997) Defining area-average parameters in meteorological models for land surfaces with mesoscale heterogeneity. J Hydrol 190:302–316
Nunez M, Oke TR (1976) Long-wave radiative flux divergence and nocturnal cooling of the urban atmosphere. II: Within an Urban Canyon. Bound-Lay Meteorol 10:121–135
Oke TR (1987) Boundary layer climates, 2nd edn. Methuen, London, p 435
Oke TR (2006) Towards better scientific communication in urban climate. Theor Appl Climatol 84:1–3
Panofsky HA, Dutton JA (1984) Atmospheric turbulence, models and methods for engineering applications. Wiley, New York 397
Pereira Filho AJ, Massambani O, Hallak R, Beneti CA (2008) On the use of a mobile XPOL weather radar for flood warning. In: International Symposium on Weather Radar and Hydrology, Grenoble, France. LTHE, Grenoble
Press WH, Flannery BP, Teukolsky SA, Vetterling WT (1989) Numerical recipes. The art of scientific computing (Fortran version). Cambridge University Press, Cambridge. ISBN 0 521 31330 9
Press WH, Flannery BP, Teukolsky SA, Vetterling WT (1992) Numerical Recipes (Fortran version). Cambridge University Press, p 702. ISBN 0-521-43064-X
Raupach MR (1992) Drag and drag partition on rough surfaces. Bound-Lay Meteorol 60:375–395
Raupach MR, Finnigan JJ (1997) The influence of topography on meteorological variables and surface-atmosphere interactions. J Hydrol 190:182–213
Raupach MR, Finnigan JJ, Brunet Y (1996) Coherent eddies and turbulence in vegetation canopies: the mixing-layer analogy. Bound-Lay Meteorol 78:351–382
Roach PJ (1972) Computational fluid dynamics. Hermosa, Albuquerque, p 446. ISBN 0-913478-05-9
Rotach MW (1995) Profiles of turbulence statistics in and above an urban street canyon. Atmos Environ 29(13):1473–1486
Roth M (2000) Review of atmospheric turbulence over cities. Q J Roy Meteor Soc 126:941–990
Roth M (2007) Review of urban climate research in (sub)tropical regions. Int J Climatol 27(14):1859–1873

Roth M, Oke T (1993) Turbulent transfer relationships over an urban surface. I: spectral characteristics. Q J Roy Meteor Soc 119:1071–1104

Roulet YA, Martilli A, Rotach MW, Clappier A (2005) Validation of an urban surface exchange parameterization for mesoscale models—1D case in a street canyon. J Appl Meteorol 44:1484–1498

Sailor DJ, Lu L (2004) A top-down methodology for developing diurnal and seasonal anthropogenic heating profiles for urban areas. Atmos Environ B-Urb 38:2737–2748

Shyy W, Udaykumar HS, Rao MM, Smith RW (1996) Computational fluid dynamics with moving boundaries. Dover, New York, p 285. ISBN 0-486-65675-6

Sorbjan Z (1986) On similarity in the atmospheric boundary layer. Bound-Lay Meteorol 34:377–397

Tennekes H (1973) A model for the dynamics of the inversion above a convective boundary layer. J Atmos Sci 30:558–581

Thom AS (1975) Momentum, mass and heat exchange of plant communities. In: Monteith JL (ed) Vegetation and the atmosphere. Academic, London, pp 57–110

Thom AS, Stewart JB, Oliver HR, Gash JHC (1975) Comparison of aerodynamic and energy budget estimates of fluxes over a pine forest. Q J R Meteor Soc 427:93–105

Unsworth MH (1975) Long-wave radiation at the ground. II. Geometry of interceptation by slopes, solids, and obstructed planes. Q J Roy Meteor Soc 101:25–34

Unsworth MH, Monteith JL (1975) Long-wave radiation at the ground. I. Angular distribution of incoming radiation. Q J Roy Meteor Soc 101:13–24

Vincendon BV, Ducrocq GM, Saulnier L, Boulloud K, Chancibault F, Habets, J Noilhan (2009) Advances of coupling the ISBA land surface model with a TOPMODEL hydrological model dedicated to Mediterranean flash floods. J Hydrometeorol (in press)

Viney NR (1991) An empirical expression for aerodynamic resistance in the unstable boundary layer. Bound-Lay Meteorol 56:381–393

von Randow C, Sa' LDA, Gannabathula SSDP, Manzi AO, Arlino PRA, Kruijt B (2002) Scale variability of atmospheric surface layer fluxes of energy and carbon over a tropical rain forest in southwest Amazonia. I. Diurnal conditions. J Geophys Res-Atmos 107(D20, LBA):29-1–29-12

von Randow C, Kruijt B, Holtslag AAM (2006) Low-frequency modulation of the atmospheric surface layer over Amazonian rain forest and its implication for similarity relationship. Agr Forest Meteorol 141:192–207